

Dynamic regulation of NOTCH1 activation and Notch ligand expression in human thymus development

María J. García-León¹, Patricia Fuentes¹, José Luis de la Pompa^{2,3} and María L. Toribio^{1,*}

ABSTRACT

T-cell development is a complex dynamic process that relies on ordered stromal signals delivered to thymus-seeding progenitors that migrate throughout different thymus microenvironments (TMEs). Particularly, Notch signaling provided by thymic epithelial cells (TECs) is crucial for T-cell fate specification and generation of mature T cells. Four canonical Notch ligands (Dll1, Dll4, Jag1 and Jag2) are expressed in the thymus, but their spatial distribution in functional TMEs is largely unknown, especially in humans, and their impact on Notch1 activation during T-lymphopoiesis remains undefined. Based on immunohistochemistry and quantitative confocal microscopy of fetal, postnatal and adult human and mouse thymus samples, we show that spatial regulation of Notch ligand expression defines discrete Notch signaling niches and dynamic species-specific TMEs. We further show that Notch ligand expression, particularly DLL4, is tightly regulated in cortical TECs during human thymus ontogeny and involution. Also, we provide the first evidence that NOTCH1 activation is induced *in vivo* in CD34⁺ progenitors and developing thymocytes at particular cortical niches of the human fetal and postnatal thymus. Collectively, our results show that human thymopoiesis involves complex spatiotemporal regulation of Notch ligand expression, which ensures the coordinated delivery of niche-specific NOTCH1 signals required for dynamic T-cell development.

KEY WORDS: Notch ligands, $\gamma\delta$ T cells, Thymus microenvironment, Human

INTRODUCTION

The thymus is the primary organ for the generation of T lymphocytes, which requires the participation of highly specialized thymic epithelial cells (TECs), located either in the cortex (cTECs) or in the medulla (mTECs), where they mediate different aspects of T-cell development (Petrie and Zúñiga-Pflücker, 2007). Multipotent progenitors derived from the embryonic liver or the postnatal bone marrow enter the thymus and undergo T-cell commitment upon activation of the Notch signaling pathway, following interaction with Notch ligands expressed by cTECs (Radtke et al., 1999; Pui et al., 1999). In mammals, Notch family members include five ligands, two from the Jagged family (Jag1 and Jag2) and three from the Delta-like family (Dll1, Dll3 and Dll4), and four receptors (Notch1-4). All

Notch ligands except Dll3 are expressed in the thymus (Felli et al., 1999; Hozumi et al., 2004), but Dll4 is the essential nonredundant ligand promoting Notch1-dependent T-cell fate specification and maturation, at least in mice (Koch et al., 2008; Hozumi et al., 2008). Two T-cell subsets are generated within the thymus from a common T-cell-committed progenitor, according to the acquisition of either the $\alpha\beta$ or the $\gamma\delta$ T-cell antigen receptor (Dudley et al., 1995; Kang and Raulet, 1997). Most Notch1-induced T-cell progenitors develop along the $\alpha\beta$ lineage, while only ~1% of total postnatal thymocytes belong to the $\gamma\delta$ T cell lineage (Offner et al., 1997).

How T-cell development proceeds within the thymus is still poorly understood, especially in humans. In mouse, $\alpha\beta$ T-cell generation involves a complex journey throughout different thymus microenvironments (TMEs) (Takahama, 2006; Petrie, 2002; Petrie and Zúñiga-Pflücker, 2007), including the thymus cortex and medulla, the corticomedullary junction (CMJ) and the mesenchymal perivascular spaces (PVS) (Lobach and Haynes, 1987). Thymocytes entering the thymus through the CMJ rapidly move along the inner cortex (IC) toward the subcapsular cortex (SCC) (Lind et al., 2001), while interacting with Notch ligands expressed on cTECs (Witt and Robins, 2005). During migration, thymocytes simultaneously progress from the most immature double-negative (DN) stage, characterized by the lack of CD4 and CD8 (CD8A – Mouse Genome Informatics) surface markers, to the CD4⁺ CD8⁺ double-positive (DP) stage (Petrie and Zúñiga-Pflücker, 2007). Arrival to the SCC coincides with the selection and expansion of DP thymocytes that have successfully rearranged a TCR β locus, a process termed β -selection (Lind et al., 2001; Hoffman et al., 1996). Then, thymocytes turn back inwards to the IC, rearrange and express TCR α , and undergo positive selection by means of TCR $\alpha\beta$ -mediated recognition of antigens expressed on cTECs, to finally reach the thymus medulla as CD4⁺ or CD8⁺ single-positive (SP) TCR $\alpha\beta$ cells. Interaction with mTECs and dendritic cells (DCs) promotes clonal deletion of autoreactive TCR $\alpha\beta$ thymocytes, induces acquisition of T-cell tolerance and results in thymus egress of SP cells to the periphery. The complex migration of $\alpha\beta$ thymocytes throughout the thymus illustrates the step-wise Notch dependency of $\alpha\beta$ T-cell development (Schmitt et al., 2004), and highlights the potential specific role that distinct TMEs expressing particular Notch ligands might play to regulate recurrent Notch signaling required for dynamic $\alpha\beta$ T-cell generation (Ciofani and Zúñiga-Pflücker, 2007; Griffith et al., 2009).

Much less is known about intrathymic $\gamma\delta$ T cell development, partly because generation of $\alpha\beta$ or $\gamma\delta$ T cells seems to involve distinct Notch activation thresholds, which also differ between mice and humans (Tanigaki et al., 2004; Garbe et al., 2006; Van de Walle et al., 2009; Garcia-Peydro et al., 2003). As distinctive Notch signaling thresholds are the result of different Notch receptor-ligand interactions (Shimizu et al., 2002; de La Coste and Freitas, 2006; Van de Walle et al., 2013), availability of particular Notch ligands at specific intrathymic niches might regulate critical developmental

¹Department of Cell Biology and Immunology, Centro de Biología Molecular Severo Ochoa, Consejo de Superior de Investigaciones Científicas (CSIC), Universidad Autónoma de Madrid (UAM), 28049 Madrid, Spain. ²Intercellular Signaling in Cardiovascular Development & Disease Laboratory, Centro Nacional de Investigaciones Cardiovasculares Carlos III (CNIC), 28029 Madrid, Spain. ³CIBER CV, 28029 Madrid, Spain.

*Author for correspondence (mtoribio@cbm.csic.es)

 M.L.T., 0000-0002-8637-0373

decisions within the thymus, including $\alpha\beta$ versus $\gamma\delta$ T-cell fate. Supporting this possibility, we have recently shown that the lymphoid versus myeloid cell fate of progenitors seeding the human thymus is specifically imposed by unique signals provided by JAG1 that promote the generation of DCs (Martin-Gayo et al., 2017). Therefore, regulation of Notch signal strength induced by specific Notch ligands in particular contexts might critically determine intrathymic cell fate outcomes. However, Notch signaling cues delivered within the thymus are not yet well documented, particularly in humans. Consequently, extensive characterization of Notch ligand-expressing thymus niches is required to comprehensively outline human T-cell development. In addition, a precise knowledge of the dynamic regulation of Notch activation and Notch ligand expression during fetal and adult life is crucial to understand how thymus homeostasis is controlled, and to decipher the molecular basis of thymic involution and immunosenescence. To approach these aims, we here have performed immunohistochemistry and confocal microscopy analyses of Notch ligand expression and NOTCH1 activation along human thymus ontogeny. We show that spatial and temporal regulation of expression of particular Notch ligands defines discrete and dynamic TMEs, which differ between humans and mice. Likewise, evidence is provided that *in vivo* induction of NOTCH1 activation in intrathymic progenitors is spatiotemporally regulated in human T-lymphopoiesis. Globally, our study reveals a tight regulation of Notch ligand expression at discrete human TMEs that might be crucial for coordinated development of human T cells.

RESULTS

Spatial regulation of Notch ligand expression in the human thymus defines specific Notch signaling niches

To gain some insights into the functional relevance of intrathymic Notch ligand expression in human T-cell development, we assessed the distribution of DLL1, DLL4, JAG1 and JAG2 ligands in the human thymus by immunohistochemical and quantitative confocal microscopy approaches. We first focused on human postnatal thymus (PNT) samples (<18 months old) (Fig. 1A-L), and specifically on the pan-cytokeratin (pCK)-positive TEC compartment, with special attention to TECs located in the thymus cortex, which is the main site of T-cell maturation (Griffith et al., 2009). We found that DLL1 was expressed in both cTECs and mTECs in the human PNT (Fig. 1A,E,I), coincident with results previously observed in mice (Hozumi et al., 2004; Koch et al., 2008; Schmitt et al., 2004) and confirmed in Fig. 2A,E,I. Rare nonepithelial cortical and medullary thymocytes (Fig. 1E,I), as well as myeloid CD11c⁺ (ITGAX⁺ – Human Gene Nomenclature Database) medullary cells characterized as DCs (Fig. 3A,C), likewise expressed DLL1. However, in contrast to mouse cTECs (Fig. 2B,F,O,P), most human postnatal cTECs lacked the essential DLL4 ligand (Fig. 1B,F). Only very scarce cTECs located at the SCC and some mTECs expressed DLL4 in the human thymus, although at low levels (Fig. 1F,J), but high DLL4 expression was displayed by myeloid medullary cells (Fig. 3D), mesenchymal PVS cells and endothelium (Fig. 3H). Notably, despite distinct frequencies of TECs positive for DLL1 or DLL4, ligands were located in the cortex and the medulla of the human PNT; similar expression levels of these ligands were found in both TEC subtypes (Fig. 1M). These results indicate that DLL4 expression is significantly reduced in cTECs in human compared with mouse PNT (Fig. 2O,P), which might suggest a species-specific role of DLL4 in postnatal T-cell development.

Regarding Jagged ligands, current mouse data indicate that Jag1 is medullary specific (Lehar et al., 2005), and we confirmed that

Jag1 is highly expressed in the medulla in the mouse PNT (Fig. 2C,K), but is essentially absent from the cortex (Fig. 2C,G,M). This selective distribution is conserved in humans, where JAG1 expression is confined to mTECs (Fig. 1C,K,M), to rare nonepithelial medullary cells characterized as DCs (Martin-Gayo et al., 2017) and also to endothelium (Fig. 3E,I). In contrast to Jag1, intrathymic Jag2 expression has been poorly addressed in the mouse thymus (Jiang et al., 1998), and no studies have been reported in humans. We thus sought to assess this issue and found that Jag2 is the most prominent cortical Notch ligand, which is confined to cTECs in both human (Fig. 1D,H,L,M) and mouse (Fig. 2D,H,L,M) PNT. Conversely, human (Fig. 1D,L,M) and mouse (Fig. 2D,L,M) mTECs display low Jag2 expression. JAG2 is likewise poorly detected in rare medullary DCs (Fig. 3F,K), but it is highly expressed in the vasculature (Fig. 3J). Therefore, in contrast to Delta-like ligands, Jag1 and Jag2 expression defines reciprocal medullary and cortical TMEs, respectively, in the human (Fig. 1M) and mouse (Fig. 2M) PNT. Interestingly, detailed image analysis and quantitative measurements of Jag2 expression in pCK-labeled cTECs located at defined regions of interest (ROIs) within the cortex showed a species-specific regulation of Jag2 expression gradients along distinct cortical niches. In humans, JAG2 is significantly enriched in cTECs located at the CMJ, but its expression decreases sequentially at the IC and SCC (Fig. 1D,N). Conversely, Jag2 is mostly expressed by SCC cTECs in mice and decreases at the CMJ (Fig. 2D,N). Therefore, reciprocal Jag2 expression gradients are displayed in the PNT cortex in mouse and human.

Nonepithelial thymic stromal cells express distinct Notch ligands at the CMJ and the medulla in human

As mentioned above, besides TECs, a significant number of nonepithelial cells morphologically distinct from thymocytes, located at the corticomedullary PVS and the medulla of the human PNT, express Notch ligands. These thymic regions are enriched in CD34⁺ mesenchymal cells and CD11c⁺ myeloid cells, respectively (Fig. 3A,B). Myeloid stromal cells were found to express all four Notch ligands although at distinct frequencies, as Delta-like ligands are prevalent in CD11c⁺ cells, whereas JAG1 and JAG2 are poorly represented (Fig. 3C-F,K). DLL4, JAG1 and JAG2, but not DLL1, are also expressed in the thymic vasculature and mesenchymal CD34⁺ cells located at the corticomedullary PVS (Fig. 3G-J). In order to provide a comprehensive picture of Notch ligand expression levels in the distinct TMEs characterized in the human PNT, we next performed quantitative analyses in single stromal cells – including cTECs, mTECs, myeloid and perivascular cells – based on colocalization profiling (Fig. S1). Collectively, our results provide evidence of a differential distribution of Notch ligands at distinct histological regions and diverse stromal cell types within the human PNT, which might define specific functional niches.

Regulation of Notch ligand expression in human thymus ontogeny and involution

The striking finding that Dll4, the essential ligand involved in murine T-cell development, is poorly expressed in cTECs in the human PNT prompted us to investigate whether expression of DLL4 is regulated during human thymopoiesis. Confirming this possibility, we found that DLL4 is expressed at higher levels in fetal cTECs (11-19 weeks of embryonic development) than in postnatal cTECs (Fig. 4B,F,J,M,N). In mice, however, Dll4 expression was similar in fetal and postnatal cTECs (Fig. 2 and data not shown), reflecting important species-specific differences in the temporal expression of cortical Dll4. In contrast to DLL4,

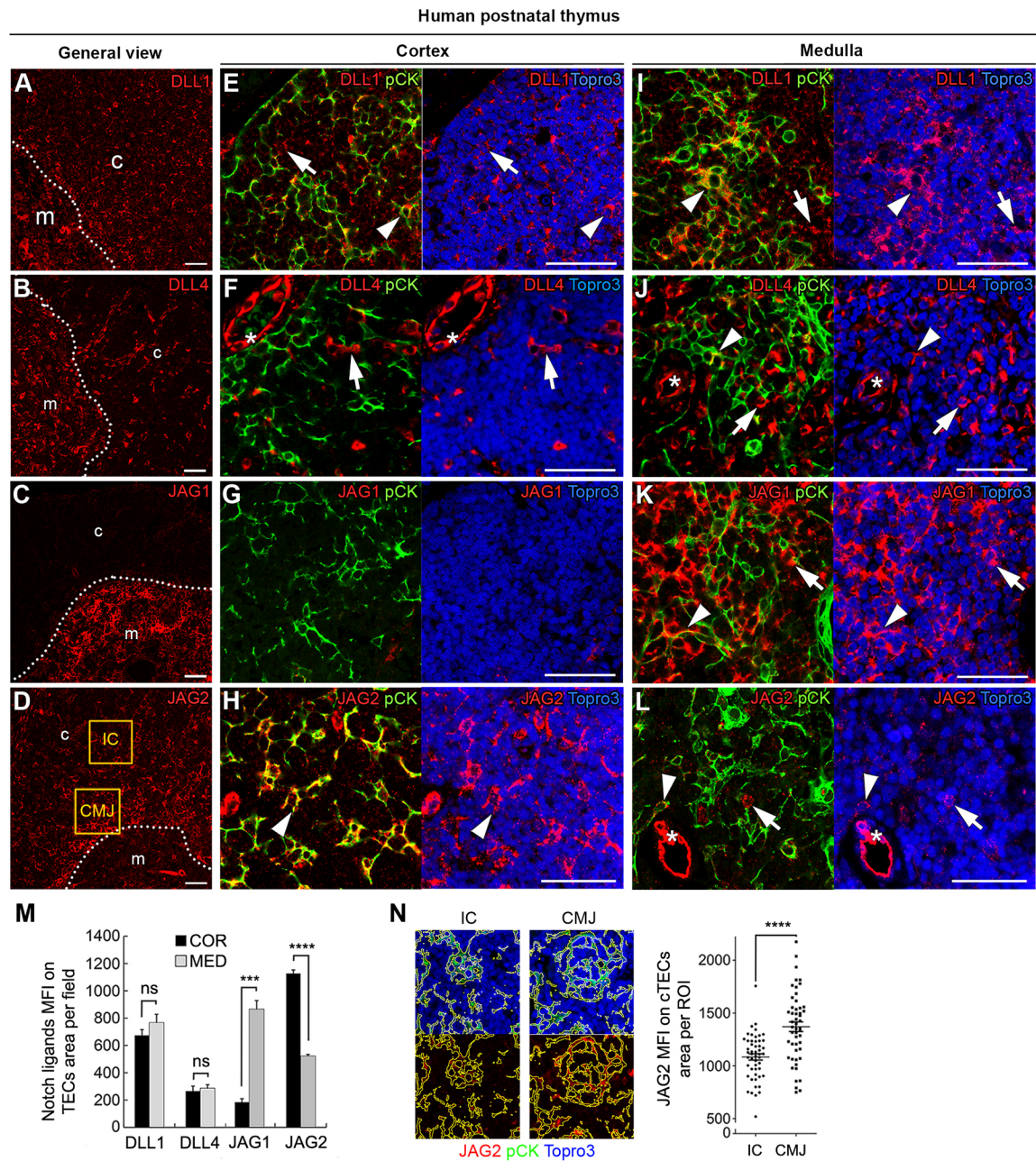


Fig. 1. Notch ligand expression pattern in the human PNT. (A-L) Immunohistochemistry of the indicated Notch ligands (red) and TECs (pCK, green). Topro3 staining shows nuclei (blue). c, cortex; CMJ, corticomedullary junction; IC, inner cortex; m, medulla. The dotted lines indicate the CMJ; asterisks indicate the endothelium. General (A-D) and detailed view of Notch ligand expression in the cortex (E-H) and medulla (I-L) in human PNT. Arrowheads indicate co-expression of Notch ligand and cytokeratins (pCK) in TECs; arrows indicate Notch ligand expression in nonepithelial cells. Scale bars: 50 μ m. Images shown are representative of at least ten images per sample ($n=3$). (M) Notch ligand expression as mean fluorescence intensity (MFI) in the cortex (COR) and medulla (MED). (N) JAG2 expression levels (MFI) in the IC and CMJ niches of the PNT (right), obtained by intensity level thresholding on pCK⁺ cells of least 30 regions of interest (ROIs) in 12-bit color depth images, from $n=3$ independent samples. ns, nonsignificant; *** $P<0.001$; **** $P<0.0001$.

DLL1, JAG1 and JAG2 expression was similar in fetal and postnatal human TECs, both in the cortex and the medulla (Fig. 4), indicating that regulation of Notch ligand expression in cTECs during human thymopoiesis is DLL4 specific. Quantitative analyses further assessed DLL4 downregulation in cTECs with age using thymus endothelium as an internal control, because DLL4 expression remains essentially constant during life in human thymic endothelial cells (ECs) (Fig. 4M), as well as in mouse thymic ECs (Hozumi et al., 2008). We found that DLL4 becomes more than 55% downregulated in postnatal compared with fetal human

cTECs (Fig. 4M,N), whereas such a decrease was not observed in mouse (Fig. 2O,P).

Next, we sought to investigate whether the expression of Notch ligands is also regulated with age in postnatal life. Expression analyses of Delta-like ligands in human thymus samples from 6- to 11-year-old individuals (referred to as adult thymus) showed no differences from those in PNT samples, except for increased expression of DLL1 in mTECs and Hassall's corpuscle cells (data not shown), as previously observed in mice (Aw et al., 2009). However, we found that JAG1 and JAG2 expression differed in adult

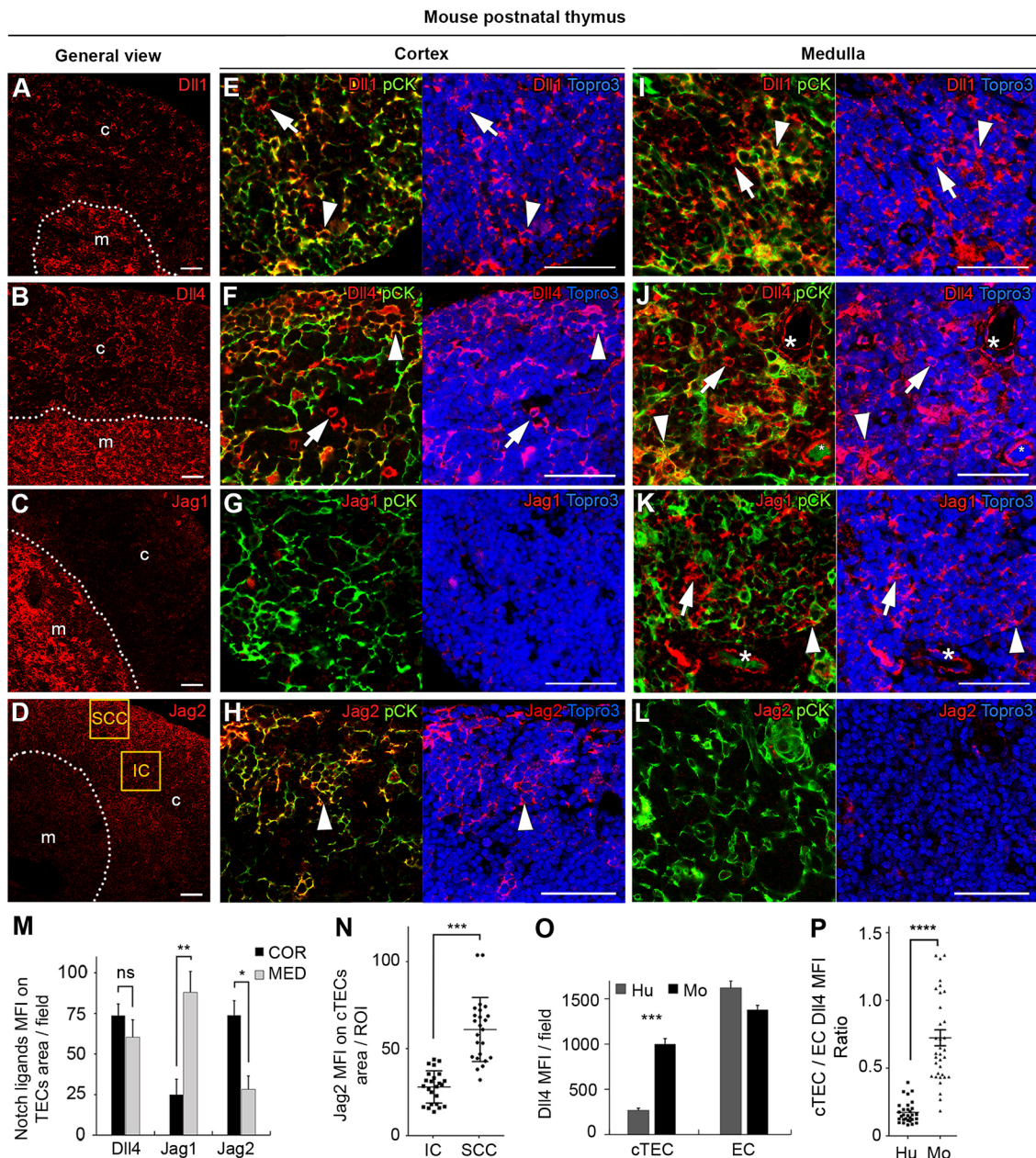


Fig. 2. Notch ligand expression in the mouse PNT. (A-L) Immunohistochemistry of the indicated Notch ligands (red) in mouse PNT (<16 weeks old). TECs are characterized by the expression of cytokeratins (pCK) (green). Topro3 staining shows nuclei (blue). c, cortex; IC, inner cortex; m, medulla; SCC, subcapsular cortex. The dotted lines indicate the CMJ; asterisks indicate the endothelium. (A-D) General view of Notch ligand distribution. (E-H) Detailed view of Notch ligand expression in the cortex. (I-L) Detailed view of Notch ligand expression in the medulla. Arrowheads indicate expression in TECs; arrows indicate expression in non-epithelial cells. Images shown are representative of results obtained from at least ten images per thymus sample ($n=2$). Scale bars: 50 μ m. (M) Notch ligand expression levels in the cortex (COR) and medulla (MED). Results are shown as MFI values \pm s.e.m., obtained from at least ten images per thymus sample ($n=2$). (N) Jag2 expression levels in cortical TECs located in the IC and SCC. Results are shown as MFI values \pm s.e.m., obtained by thresholding (green) from at least 30 ROIs selected at the IC and SCC from ten images per thymus sample ($n=2$). (O) Dll4 expression levels displayed by TECs and endothelial cells (EC) located at the cortex in human (Hu) and mouse (Mo) PNT. (P) Relative Dll4 expression in cTEC normalized to expression in EC in human and mouse PNT. Results are shown as MFI values from at least ten images per thymus sample ($n=2$). ns, nonsignificant; * $P<0.05$; ** $P<0.01$; *** $P<0.001$; **** $P<0.0001$.

compared with postnatal human cTECs (Fig. 5). Quantitative assays revealed that the JAG2 decreasing gradient observed from the CMJ to the IC of the human PNT (Fig. 1N) is lost in the adult thymus, likely as a result of age-dependent downregulation of JAG2 at the CMJ (Fig. 5I,J). Also, we found that JAG1, but not JAG2, expression was significantly upregulated with age in cTECs at the SCC, as assessed by normalization to invariant expression in ECs (Fig. 5E-H,K). Collectively, our results showing the downregulation of DLL4 expression in cTECs in the human PNT, together with the age-

associated upregulation of JAG1 at the SCC and the disappearance of the cortical JAG2 expression gradient, provide evidence of a spatiotemporal regulation of Notch ligand expression in cTECs in the human thymus.

NOTCH1 activation is induced *in vivo* in CD34⁺ progenitors resident in the human thymus cortex

To determine the functional relevance of the dynamic Notch ligand-expressing niches identified in the human thymus, we next analyzed

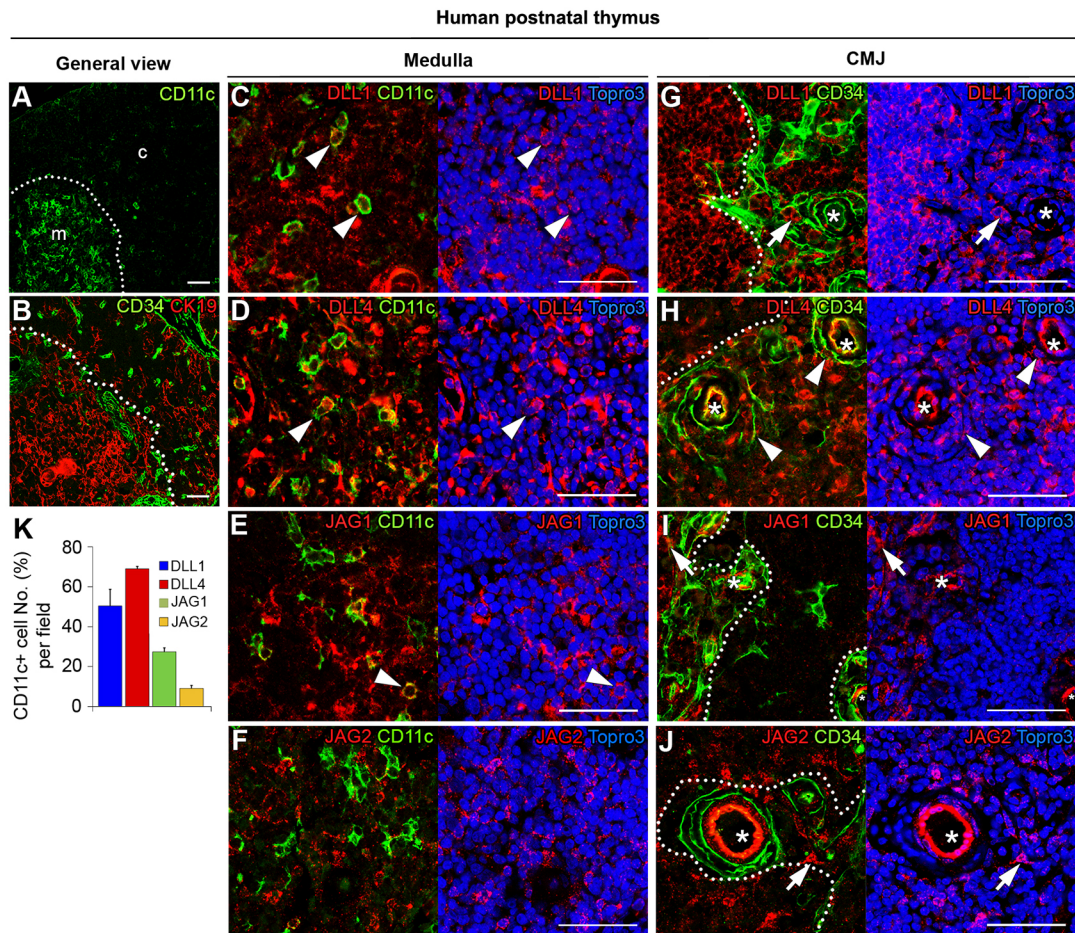


Fig. 3. Nonepithelial thymic stromal cells differentially express Notch ligands at the CMJ and the medulla in human. (A–J) Immunohistochemistry of the indicated Notch ligands (red) in human PNT. Stromal myeloid and PVS cells are characterized by expression of CD11c or CD34 (green), respectively. Topro3 staining shows nuclei (blue). c, cortex; m, medulla. The dotted lines indicate the CMJ; asterisks indicate the endothelium. (A, B) General view of CD11c and CD34 expression. The PVS niche is defined as CK19⁻ (KRT19⁻) CD34⁺. (C–F) Notch ligand expression in myeloid CD11c⁺ stromal cells of the medulla. (G–J) Notch ligand expression in CD34⁺ mesenchymal cells. Arrowheads indicate co-expression of Notch ligands with CD11c or CD34; arrows indicate expression in CD34⁻ perivascular cells. (K) Frequencies of medullary myeloid CD11c⁺ stromal cells expressing Notch ligands. Results are shown as mean percentages \pm s.e.m., per 63 \times field from at least ten images obtained from different tissue samples ($n=3$). Scale bars: 50 μ m.

Notch activation *in situ* by immunohistochemistry using a monoclonal antibody specific for the active intracellular form of NOTCH1 (ICN1). Cells expressing active NOTCH1 were essentially absent in the human PNT medulla, although scarce ICN1⁺ cells morphologically distinct from thymocytes were observed (Fig. 6A and data not shown). However, we identified a significant number of ICN1⁺ cells distributed throughout distinct regions of the thymic cortex (Fig. 6A, L). Co-expression analyses of ICN1 and pCK indicated that such ICN1⁺ cells were thymocytes located in close contact with cTECs in all cortical regions, including the SCC, IC and CMJ (Fig. 6B–D). Notably, ICN1⁺ thymocytes were significantly enriched at the CMJ and SCC (Fig. 6L), two intrathymic regions in which critical NOTCH1-dependent T-cell developmental checkpoints take place (Petrie and Zúñiga-Pflücker, 2007). In addition, rare isolated ICN1⁺ cells were found in PVS at the CMJ (Fig. S2A, B), suggesting that thymocyte progenitor traffic through extraparenchymal areas. To further characterize the nature of the main population of ICN1⁺ cortical thymocytes, we analyzed the co-expression of ICN1 and the hematopoietic progenitor cell marker CD34 in PNT samples. We found that most ICN1⁺ cortical thymocytes lacked or expressed very low levels of CD34, suggesting that they have downregulated CD34 as

a consequence of induced T-cell commitment. However, we found that more immature CD34⁺ progenitors were enriched at the CMJ, and some were also identified in the IC and SCC (Fig. 6E–K). Notably, all CD34⁺ progenitors co-expressed active NOTCH1 (Fig. 6I–K), thus providing formal evidence that NOTCH1 activation is induced *in vivo* in human CD34⁺ progenitors and is involved in early human T-cell development. Collectively, these results allowed us to identify *in situ* the functional niches that support NOTCH1 signaling in the human PNT.

As expression of Notch ligands, particularly DLL4, is temporally regulated during human thymus development, we next investigated whether DLL4 downregulation has an impact on NOTCH1 signaling during human thymopoiesis. To this end, we compared the pattern of *in vivo* NOTCH1 activation in the PNT (Fig. 6) and in the fetal and adult thymus (Fig. 7). We found that, similarly to the ICN1⁺ pattern observed in the PNT, ICN1⁺ thymocytes were present in the cortex in fetal (Fig. 7A–D), as well as adult (Fig. 7E–H), thymus, although at significantly distinct frequencies (Fig. 7K). Numbers of ICN1⁺ cortical thymocytes were significantly higher in the fetal thymus than in the PNT, and decreased markedly in the adult thymus, indicating that intrathymic NOTCH1 activation

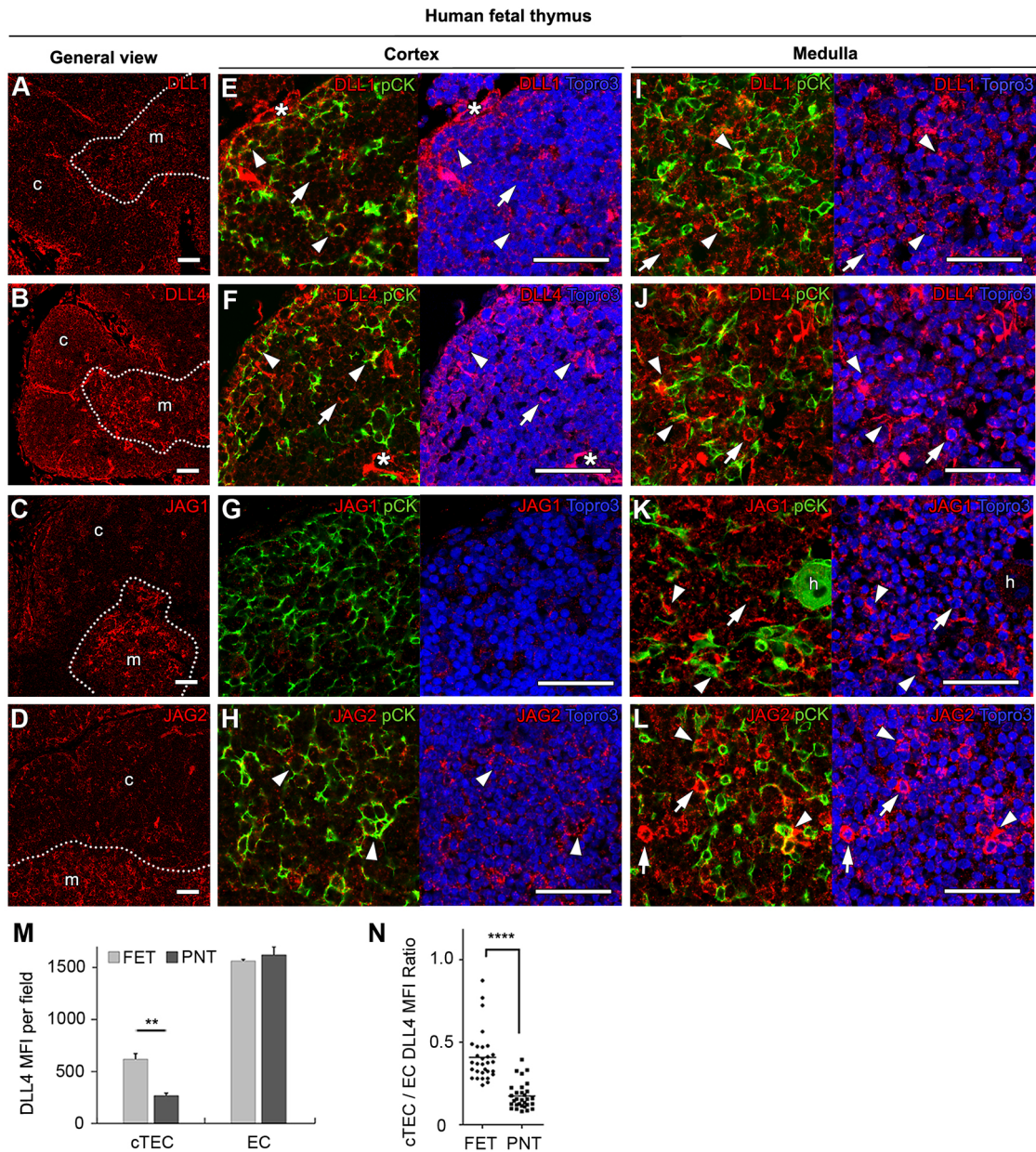


Fig. 4. Notch ligand expression pattern in the human fetal thymus. (A-L) Immunohistochemistry of the indicated Notch ligands (red) and TECs (pCK) (green). Topro3 staining shows nuclei (blue). c, cortex; h, Hassall's corpuscle; m, medulla. The dotted lines indicate the CMJ; asterisks indicate the endothelium. General (A-D) and detailed view of Notch ligand expression in the cortex (E-H) and medulla (I-L) in the human fetal thymus. Arrowheads indicate co-expression of Notch ligand and cytokeratins (pCK) in TECs; arrows indicate Notch ligand expression in nonepithelial cells. Scale bars: 50 μ m. Images shown are representative of at least ten images per sample ($n=3$). (M) DLL4 expression levels (MFI) displayed by cortical TECs (cTEC) and endothelial cells (EC) located in fetal (FET) and postnatal (PNT) thymus. MFI levels were obtained by intensity level thresholding as shown previously. (N) Relative DLL4 expression in cTEC normalized to expression in EC of values in M. Results are representative of at least ten images per sample ($n=3$). DLL4 images were acquired in 12-bit color depth with the same nonsaturating settings. ** $P<0.01$; **** $P<0.0001$.

decreases with age in humans. Moreover, we observed age-associated changes in the distribution of ICN1⁺ thymocytes at particular cortical niches, as they accumulated in the SCC in the fetal and adult thymus (Fig. 7I,J), but were also enriched at the CMJ region of the PNT (Fig. 6L). Thymocytes expressing active NOTCH1 were also detected at extraparenchymal regions in the fetal thymus, mostly at the mesenchymal interlobular spaces (Fig. S2C,D), in contrast to extraparenchymal postnatal thymocytes, which localized to the PVS (Fig. S2A,B). Collectively, our data provide formal evidence that numbers of thymocytes undergoing NOTCH1 activation and T-cell

specification decrease significantly with age in human thymus ontogeny and postnatal life, a finding that correlates with significant changes in the localization of developing thymocytes receiving NOTCH1 activation signals.

DISCUSSION

T-cell development is a dynamic tightly regulated process involving the migration of developing thymocytes throughout different thymus niches that provide stage-specific developmental cues (Petrie and Zúñiga-Pflücker, 2007). Recurrent Notch receptor-ligand interactions in the thymus are crucial in this process (Schmitt et al., 2004),

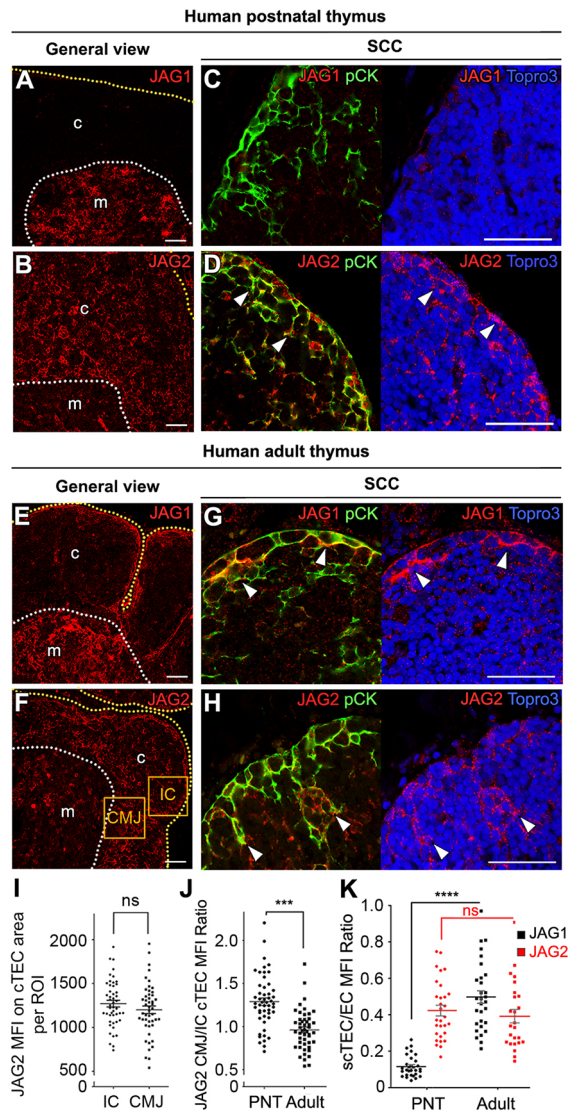


Fig. 5. Age-dependent regulation of JAG1 and JAG2 expression on TECs located at distinct cortical regions in the human thymus.

(A-H) Immunohistochemistry of the indicated Notch ligands (red) and TECs (pCK) (green). Topro3 staining shows nuclei (blue). General (left column) and detailed view of the subcapsular cortex (SCC, right column) in postnatal (A-D) and adult (E-H) thymus. c, cortex; CMJ, corticomedullary junction; IC, inner cortex; m, medulla. White dotted lines indicate the CMJ; yellow dotted lines indicate the thymic capsule; asterisks indicate the endothelium. Arrowheads indicate cTECs in the SCC expressing JAG1 or JAG2 ligands. Images shown are representative of at least ten images per sample ($n=2$). Scale bars: 50 μm . (I) JAG2 expression levels (MFI) in IC and CMJ cTECs in the adult thymus. (J) Relative JAG2 expression in cTECs at the CMJ normalized to expression in the IC in postnatal (PNT) and adult thymus. Results are shown as MFI values from at least 45 ROIs selected from more than ten images per sample ($n=2$). (K) JAG1 and JAG2 expression in SCC TECs normalized to EC expression in PNT and adult thymus. SCC TEC and EC MFI values were obtained by image thresholding from at least 45 ROIs from more than ten images per PNT ($n=3$) or adult ($n=2$) thymus sample. All images were acquired in 12-bit color depth with the same nonsaturating settings. ns, nonsignificant; *** $P<0.001$; **** $P<0.0001$.

indicating that expression of Notch ligands by TECs might be subjected to strict regulatory mechanisms that ensure specific functions at defined intrathymic niches. Immunohistochemistry and quantitative confocal microscopy were used in this study to identify such niches in humans, providing a comprehensive view of the

dynamic expression of distinct Notch ligands at defined compartments within the human thymus, which highlights important differences from the mouse thymus. Formal proof is also provided for the first time that NOTCH1 activation occurs *in vivo* in developing thymocytes, which allows tracing T-cell fate specification at particular niches of the human fetal and PNT. Moreover, we show that temporal regulation of Notch ligand expression defines species-specific TMEs during human thymus ontogeny and involution.

It is well established that Notch1 signaling required for T-cell commitment and differentiation of thymus-seeding progenitors (Radtke et al., 1999; Pui et al., 1999) critically relies on Notch1-Dll4 interactions in mice (Hozumi et al., 2008; Koch et al., 2008), and this signaling axis also seems to be crucial in humans (Van de Walle et al., 2009, 2011). Therefore, the differential expression of Dll4 in mouse and human postnatal cTECs was somewhat unexpected. Importantly, we observed that although DLL4 was weakly expressed in human cTECs, its expression was significantly high in the embryonic thymus, particularly during the 11-19 weeks ontogenic window analyzed here, thus indicating that DLL4 is actively downregulated in human thymus ontogeny before birth, whereas such a decrease was not observed in the mouse PNT (not shown). However, Dll4 expression decreases dramatically in the adult mouse thymus as a result of specific cTEC-DP thymocyte crosstalk (Fiorini et al., 2008). Considering that human fetal ontogeny is proportionally accelerated compared with that of mouse, it is conceivable that Dll4 downregulation is induced earlier in human than in mouse thymopoiesis, probably during the second third of gestation, when the full T-cell repertoire and the definitive postnatal thymic configuration have been established (Lobach and Haynes, 1987; Haynes et al., 2000). Therefore, Dll4 might be functionally relevant in terms of T-cell development at earlier ontogenic stages in human compared with mouse thymus.

The observed downregulation of DLL4 during human thymus development concurs with the fact that T-cell generation progressively decreases with age in human postnatal life (O'Neill et al., 2016). In fact, the thymus is the first organ to degenerate during normal aging, a process termed thymic involution, which correlates with the appearance of severe histological and molecular changes and results in impaired T-cell generation and immunosenescence (Haynes et al., 2000; Chinn et al., 2012). Accordingly, we found a dramatic decrease in thymocytes receiving NOTCH1 activation signals in adult compared with postnatal and fetal human thymus stages. In the adult thymus, this decrease concurs with the loss of a specific localization of ICN1⁺ thymocytes, in particular TMEs, such as the SCC and the CMJ, and with a marked disorganization of Notch ligand expression, characteristic of thymus involution. Given that DLL4 is the most affected ligand in thymus aging, a direct functional association between DLL4 downregulation and human thymus involution could be established. Regarding the mechanism responsible for age-dependent Dll4 downregulation in the thymus, it is known that Dll4 expression in TECs is induced by the transcription factor FOXN1 (Calderón and Boehm, 2012), which is a master regulator of TEC function and T-cell development. Studies in mice, later confirmed in humans, have shown that FOXN1 is downregulated with age in the thymic stroma at the onset of thymic involution (Ortman et al., 2002; Reis et al., 2015), coincident with the loss of Dll4 (O'Neill et al., 2016). These data suggest that dynamic regulation of FOXN1 leads to thymic involution, partly owing to Dll4 downregulation. Thus, the early emergence of thymic involution in human life highlights the relevance of the embryonic thymus in the process of T-cell development and mature T-cell repertoire establishment.

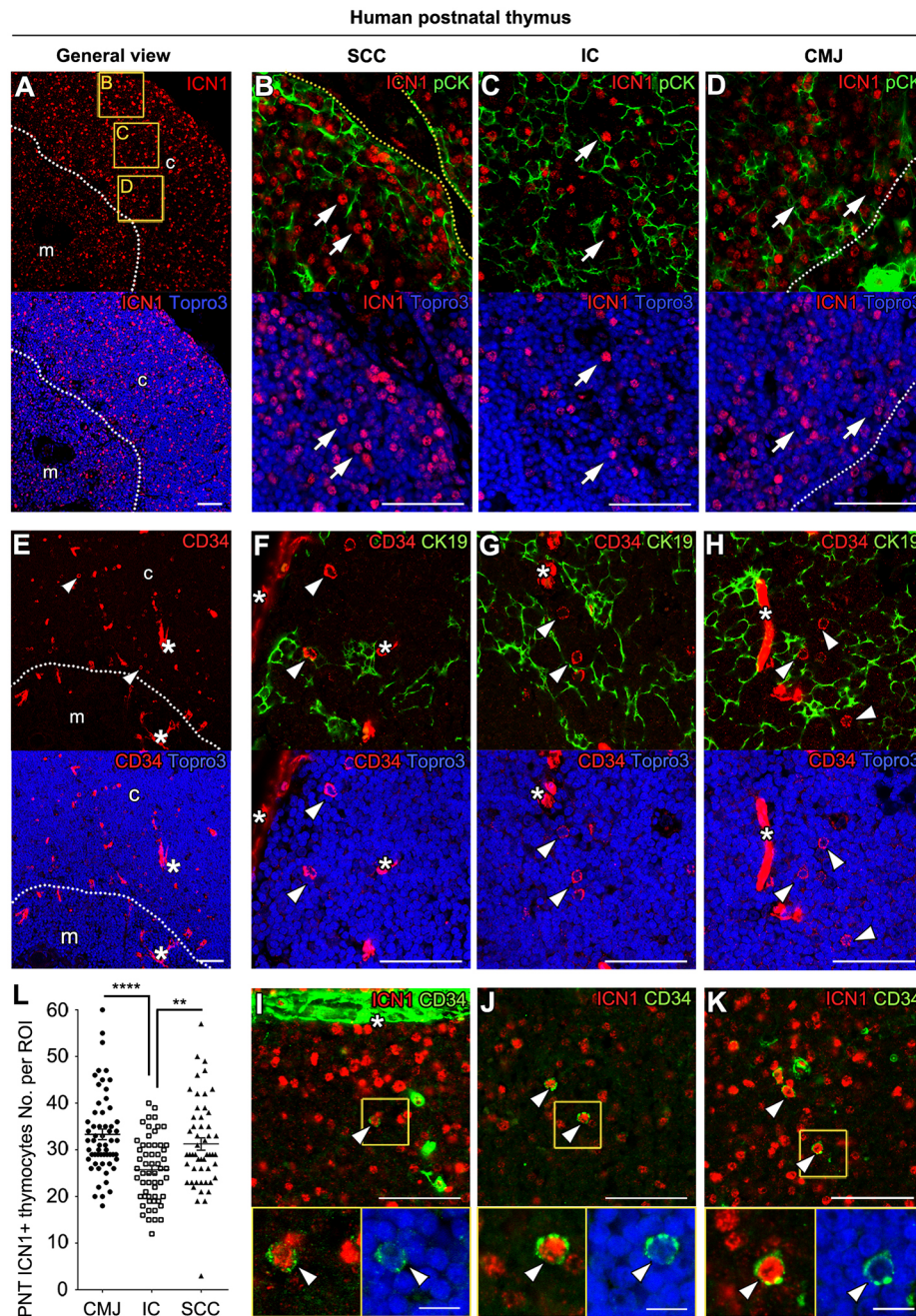


Fig. 6. Identification of *in vivo* NOTCH1 activation in cortical thymocytes and CD34⁺ progenitors located in the SCC, IC and CMJ of the human PNT. (A-K) Immunohistochemistry of active intracellular NOTCH1 (ICN1, red) or CD34 (red or green) and pCK (green), with nuclei in blue (Topro3). c, cortex; CMJ, corticomedullary junction; IC, inner cortex; m, medulla; SCC, subcapsular cortex. White dotted lines indicate the CMJ; yellow dotted lines indicate the thymic capsule; asterisks indicate the endothelium. General (A,E) and detailed view of the SCC (B,F,I), IC (C,G,J) and CMJ (D,H,K) cortical regions of the human PNT. Arrowheads indicate ICN1 or CD34 expression in thymocytes. (I-K) Arrowheads show cortical CD34⁺ thymocytes expressing nuclear ICN1. Scale bars: 50 μm (10 μm in insets). (L) Total numbers of ICN1⁺ thymocytes per region in the PNT. Images and data are representative of values from at least 15 ROIs selected from more than ten images per thymus sample (n=3). **P<0.01; ****P<0.0001.

Although Dll4 expression is markedly downregulated with age in cTECs, postnatal Dll4 expression remains high in the cortical endothelium and the PVS region. This finding is compatible with a role of non-TEC niches in T-cell fate specification, as bone marrow-derived progenitors should face Dll4 when entering the PNT by endothelial extravasation. Moreover, immediately after extravasation, thymic immigrants localize within the Dll4-enriched PVS, which represents the main gate for thymus entry (Petrie and Zúñiga-Pflücker, 2007). Consequently, nonepithelial Dll4-expressing niches could support Notch1-dependent T-cell priming. According to this possibility, we found that rare ICN1⁺ cells of lymphoid morphology are present in the PVS of the human PNT. However, most postnatal ICN1⁺ progenitors localize at the CMJ and SCC regions, suggesting that regardless of the thymus entry site, expansion and differentiation of postnatal thymocytes occurs in the CMJ and SSC regions, the specific compartment in

which T-cell developmental checkpoints take place (Petrie and Zúñiga-Pflücker, 2007). Notably, essentially all human ICN1⁺ thymocytes located at the CMJ were CD34⁺ progenitors, a finding compatible with the possibility that Notch ligands distinct from DLL4 expressed at the CMJ, like JAG2, could promote T-cell commitment and development when DLL4 becomes downregulated, whereas Jag2 would be unable to replace Dll4 function in mice (Hozumi et al., 2008; Koch et al., 2008). Alternatively, low Dll4 expression levels displayed by postnatal TECs at the CMJ might be sufficient to trigger T-cell lineage commitment, and Dll4 expression in mice (Maillard et al., 2006). The distribution of ICN1⁺ cells in the human PNT differed from that in the fetal thymus, where ICN1⁺ thymocytes preferentially accumulate at the Dll4-enriched SCC, although some ICN1⁺ cells are also located at the interlobular capsule region. This selective localization suggests that, during the

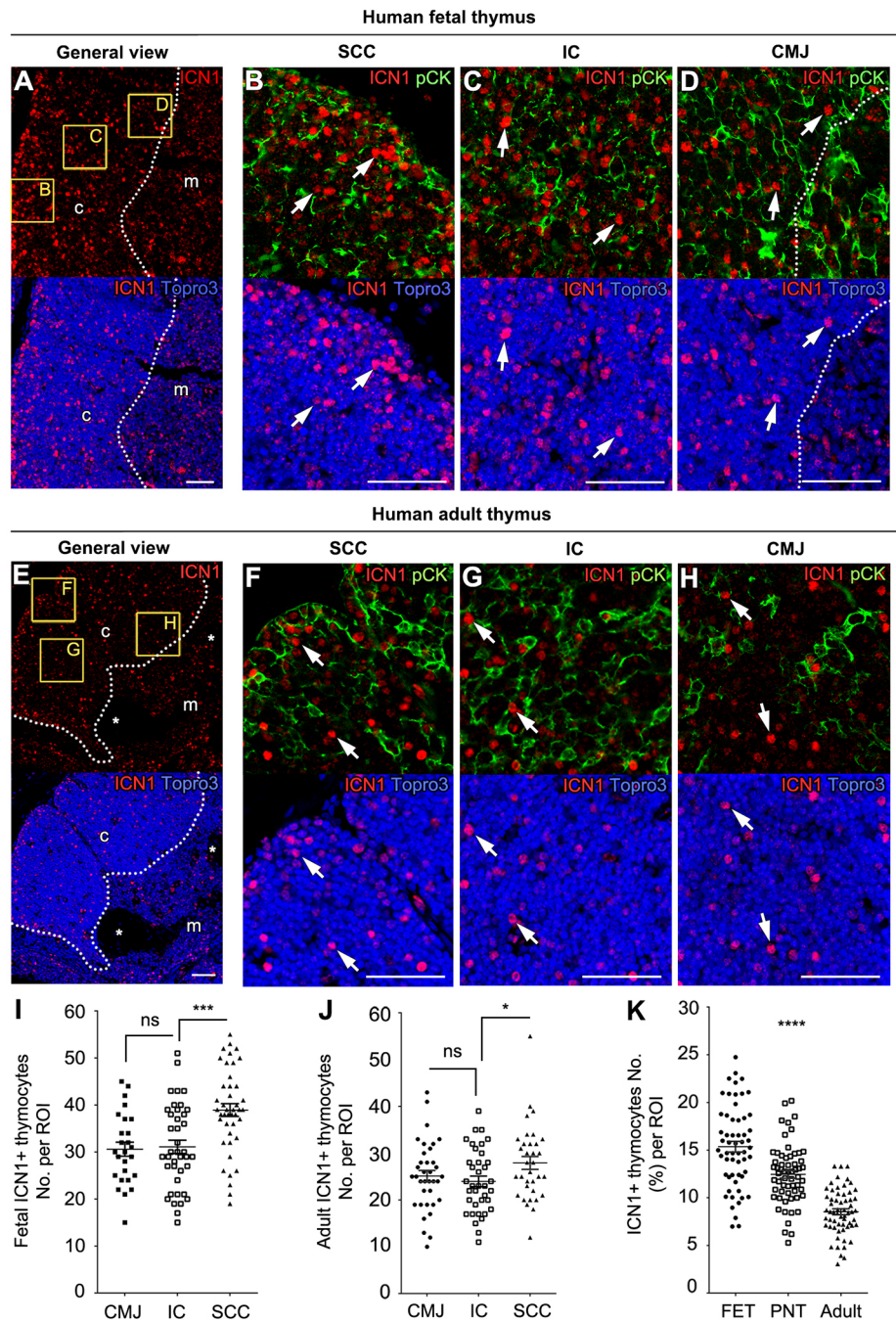


Fig. 7. Identification of *in vivo* NOTCH1 activation in cortical thymocytes located at the SCC, IC and CMJ of the human fetal and adult thymus. (A-H) Immunohistochemistry of active intracellular NOTCH1 (ICN1, red) and pCK (green), with nuclei in blue (Topro3). c, cortex; CMJ, corticomedullary junction; IC, inner cortex; m, medulla; SCC, subcapsular cortex. White dotted lines indicate the CMJ; yellow dotted lines indicate the thymic capsule; asterisks indicate the endothelium. General (A,E) and detailed view (B-D,F-H) of ICN1 expression in human fetal (A-D) and adult (E-H) thymus. Arrows indicate ICN1 expression in thymocytes. Scale bars: 50 μ m. (I,J) Total numbers of ICN1⁺ thymocytes per region in human fetal (I) and adult (J) thymus. (K) Relative number (%) of total cortical ICN1⁺ thymocytes along human thymus ontogeny [fetal (FET), postnatal (PNT) and adult]. Thymocyte numbers were obtained by counting total Topro3⁺ nuclei and pCK⁻ ICN1⁺ cortical cells in no less than ten SCC, IC and CMJ ROIs from *n*=3 thymus samples. ns, nonsignificant; **P*<0.05; ****P*<0.001; *****P*<0.0001.

particular embryonic window analyzed in this study (11-19 weeks), thymus immigrants could enter the fetal thymus through the mesenchymal tissue that surrounds the epithelial parenchyma, which is the main thymus entry region during the early avascular period of thymus development (Haynes and Heinly, 1995), whereas the CMJ becomes the main thymus entry site when vascularization is later established.

In addition to DLL4, our findings show that DLL1 is also expressed at low levels in the human PNT. In contrast, JAG2 is highly expressed at the CMJ but decreases significantly in the IC, whereas JAG1 is essentially absent in the cortex, but defines a specific niche in the medulla, which is conserved in the mouse. Considering that the thymic IC hosts low numbers of TECs, a major cortical area of the human PNT displays very low density of Notch ligands.

Consequently, ICN1⁺ thymocyte numbers are significantly reduced in the IC compared with the CMJ at all thymus ages analyzed. This concurs with the observation that, following T-cell commitment and β -selection at the SCC niche, developmental progression along the $\alpha\beta$ T-cell lineage is strictly dependent on Notch signaling release (Van de Walle et al., 2009), and takes place during migration through the IC back to the CMJ. Conversely, strong Notch signaling favors human $\gamma\delta$ T-cell development (Garcia-Peydro et al., 2003; Van de Walle et al., 2011, 2013). In mouse, however, $\alpha\beta$ T-cell fate specification and further development needs continuous Notch signaling (Schmitt et al., 2004; Ciofani et al., 2006), which could be provided in the postnatal murine thymus by Dll4 and Dll1 expressed throughout the IC up to the SCC. Notably, although all these Notch ligands are also expressed in the human fetal thymus,

Jag2 displays an inverse expression gradient from the CMJ through the IC to the SCC in the murine and human thymus, which further illustrates that spatial regulation of Notch ligand expression defines dynamic species-specific TMEs. A hierarchy of signaling strengths induced through NOTCH1 has been proposed, with DLL4 being the stronger activator, followed closely by DLL1 and JAG2, and finally by JAG1 (Van de Walle et al., 2011). In this scenario, expression of DLL4 at the CMJ would be unable to support progression of human T-cell progenitors along the $\gamma\delta$ T-cell lineage. Conversely, JAG2 expression at the CMJ could provide the critical niche that fosters human $\gamma\delta$ T-cell development. Accordingly, seminal work by the Taghon group has shown that JAG2-mediated signaling is crucial for human $\gamma\delta$ T-cell development, but impairs $\alpha\beta$ T-cell development, at least *in vitro* (Van de Walle et al., 2013). Therefore, the differential availability of distinct Notch ligands in particular intrathymic niches might critically shape key thymocyte developmental decisions, such as $\alpha\beta$ versus $\gamma\delta$ T-cell development, at least in the human thymus. Supporting this view, we have recently shown that the restricted expression of JAG1 in the human thymus medulla controls the critical lymphoid versus myeloid developmental choice in the human thymus (Martin-Gayo et al., 2017). Collectively, our study points to the differential and dynamic regulation of Notch ligand expression in particular intrathymic niches as the critical mechanism that shape thymocyte developmental decisions and allows for the coordinated generation of distinct intrathymic cell types.

MATERIALS AND METHODS

Histology and immunohistochemistry

Human thymus biopsies were obtained from postnatal (3 day- to 17-month-old) or adult (6- to 15-year-old) patients undergoing corrective cardiac surgery, after informed consent was provided in accordance with the Declaration of Helsinki. Experiments were performed in accordance with approved guidelines established by the Research Ethics Board of the Spanish Research Council (CSIC). Murine thymus samples were obtained from 5- to 16-week-old C57BL/6 mice. Tissue samples were fixed [4% paraformaldehyde/phosphate buffered saline (PBS), Sigma-Aldrich] and paraffin embedded (Paraplast Plus, Sigma-Aldrich). Formalin-fixed paraffin-embedded (FFPE) human fetal thymic samples (11-19 weeks of gestation) were kindly provided by Dr N. Torán (Vall d'Hebron University Hospital, Barcelona, Spain). From all tissue-embedded specimens, serial 8 μ m sections were obtained and mounted on poly-lysine-coated slides (SuperFrost UltraPlus, Thermo Fisher Scientific). Tissue antigens were retrieved in FFPE slides by boiling in sodium citrate (10 mM, pH 6.0). Endogenous peroxidase activity was quenched using 1% H₂O₂ 100% methanol. For blocking unspecific antibody binding sites, samples were incubated for 1 h in blocking solution (3% bovine serum albumin, 20 mM MgCl₂, 0.3% Tween 20, 5% fetal bovine serum in PBS). Background and nonspecific staining was determined by incubating with IgG isotype-matched controls or in the absence of primary antibody (Fig. S3). Prior to the addition of secondary antibodies, tissue endogenous biotin was quenched with Avidin/Biotin blocking solutions (Vector Laboratories). For Dll4, Jag1 and Jag2 signal detection, tissue slides were incubated with a horseradish peroxidase (HRP)-coupled anti-rabbit IgG secondary antibody (DAKO) and the signal was amplified using a Cyanine-3 Tyramide Signal Amplification (TSA-Cy3) Kit (NEL 744, 25 Perkin Elmer). For Dll1 and cleaved Notch1 (ICN1) signal detection, biotinylated anti-rabbit or anti-goat IgG secondary antibody (Vector Laboratories) was added before signal amplification with an Avidin/Biotin-HRP complex (Elite Vectastain ABCComplex Kit, Vector Laboratories) and TSA-Cy3 Kit. For CK19 and pCK signal detection, Alexa Fluor dye-conjugated secondary antibodies were used (Thermo Fisher Scientific). For CD34 signal detection, a biotinylated IgG anti-mouse antibody (Vector Laboratories) was used followed by incubation with Avidin/Biotin-HRP complex. ABC-amplified signal was developed by adding Alexa Fluor 488- or Alexa Fluor 555-conjugated streptavidin (Thermo

Fisher Scientific). In all cases, nuclei were stained with Topro3 (Thermo Fisher Scientific) and slides mounted with Fluoromount-G (SouthernBiotech).

Immunohistochemistry antibodies

For immunohistochemical assays, antibodies against the following human Notch signaling components were used: DLL1 (rabbit IgG, Abcam, 1:1000), DLL4 (H-70, Santa Cruz Biotechnology, 1:50), JAG1 (28H8, Cell Signaling Technology, 1:100), JAG2 (C83A8, Cell Signaling Technology, 1:100), cleaved Notch1 (D3B8, Cell Signaling Technology, 1:50). For thymic stromal cell characterization the following antibodies were used: anti-cytokeratin 19 (rabbit IgG, Sigma-Aldrich, 1:200), anti-pan-cytokeratin (mouse IgG, Sigma-Aldrich, 1:100), anti-CD11c (5D11, Novocastra, 1:100) and anti-CD34 (My10, Beckton Dickinson, 1:100). Secondary antibodies used were: goat anti-mouse IgG1-Alexa Fluor 488 (Thermo Fisher Scientific, 1:100), donkey anti-mouse IgG2a-Alexa Fluor 555 (Thermo Fisher Scientific, 1:100) and donkey anti-rabbit IgG-Alexa Fluor 488 (Thermo Fisher Scientific, 1:100).

Acquisition and analysis of confocal microscopy images

Images were acquired using an LSM510 laser scan confocal microscope (Zeiss) coupled to an Axio Imager.Z1 or an Axiovert 200 (Zeiss) microscope using the following magnifications (Zeiss): 25 \times Plan-Neofluar [oil (NA 0.8)], 40 \times Plan-Neofluar [oil (NA 1.3)] and 63 \times Plan-Apochromat [oil (NA 1.4)]. Images were processed using ImageJ and Adobe Photoshop CS4 software, and brightness and contrast were adjusted equally in samples and controls. For mean fluorescence intensity (MFI) quantification purposes, all images were acquired in 12-bit color depth and with the same nonsaturating settings. Co-expression and MFI analyses were performed in ImageJ by selecting ROIs using intensity level threshold in the cell populations of interest. Mander's colocalization coefficients were obtained with the Intensity Correlation Analysis (ICA) plugin (http://www.uhnresearch.ca/facilities/wcif/imagej/colour_analysis.htm). Cell counting was performed in Adobe Photoshop CS4.

Statistics

Statistical analysis was performed with GraphPad Prism 6 Software. The normal distribution of the data was tested using the Shapiro–Wilk normality test. When comparing two means of normal data, statistical significance was determined by the unpaired two-tailed Student's *t*-test. When comparing more than two groups of normal data, one-way ANOVA was used. When comparing two means of non-normal data, statistical significance was determined by the unpaired Mann–Whitney test. In all cases, the α -level was set at 0.05. Data in graphs are presented as mean \pm s.e.m.

Acknowledgements

We thank Dr Nuria Torán (Banco de Teixits Fetals, Servei d'Anatomia Patològica, Hospital Universitari Vall d'Hebron, Barcelona, Spain) for fetal human thymus samples and Juan Alcain for technical support.

Competing interests

The authors declare no competing or financial interests.

Author contributions

Conceptualization: M.J.G.-L., M.L.T.; Methodology: M.J.G.-L., P.F., J.L.d.I.P.; Validation: M.L.T.; Formal analysis: M.J.G.-L., P.F.; Investigation: M.J.G.-L., P.F.; Resources: J.L.d.I.P., M.L.T.; Writing - original draft: M.J.G.-L.; Writing - review & editing: M.L.T.; Supervision: M.L.T.; Funding acquisition: J.L.d.I.P., M.L.T.

Funding

This work was supported by Ministerio de Ciencia e Innovación [SAF2013-44857-R, SAF2014-62233-EXP and SAF2016-75442-R to M.L.T.], Centros de Investigación Biomédica en Red [CB16/11/00399 to J.L.d.I.P.], Seventh Framework Programme [ThymiStem 602587 to M.L.T.] and Ministerio de Ciencia e Innovación [AP2007-01886 to M.J.G.-L.].

Supplementary information

Supplementary information available online at <http://dev.biologists.org/lookup/doi/10.1242/dev.165597.supplemental>

References

- Aw, D., Taylor-Brown, F., Cooper, K. and Palmer, D. B. (2009). Phenotypical and morphological changes in the thymic microenvironment from ageing mice. *Biogerontology* **10**, 311-322.
- Calderón, L. and Boehm, T. (2012). Synergistic, context-dependent, and hierarchical functions of epithelial components in thymic microenvironments. *Cell* **149**, 159-172.
- Chinn, I. K., Blackburn, C. C., Manley, N. R. and Sempowski, G. D. (2012). Changes in primary lymphoid organs with aging. *Semin. Immunol.* **24**, 309-320.
- Ciofani, M. and Zúñiga-Pflücker, J. C. (2007). The thymus as an inductive site for T lymphopoiesis. *Annu. Rev. Cell Dev. Biol.* **23**, 463-493.
- Ciofani, M., Knowles, G. C., Wiest, D. L., von Boehmer, H. and Zúñiga-Pflücker, J. C. (2006). Stage-specific and differential notch dependency at the alphabeta and gammadelta T lineage bifurcation. *Immunity* **25**, 105-116.
- de La Coste, A. and Freitas, A. A. (2006). Notch signaling: distinct ligands induce specific signals during lymphocyte development and maturation. *Immunol. Lett.* **102**, 1-9.
- Dudley, E. C., Girardi, M., Owen, M. J. and Hayday, A. C. (1995). Alpha beta and gamma delta T cells can share a late common precursor. *Curr. Biol.* **5**, 659-669.
- Felli, M. P., Maroder, M., Mitsiadis, T. A., Campese, A. F., Bellavia, D., Vacca, A., Mann, R. S., Frati, L., Lendahl, U., Gulino, A. et al. (1999). Expression pattern of notch1, 2 and 3 and Jagged1 and 2 in lymphoid and stromal thymus components: distinct ligand-receptor interactions in intrathymic T cell development. *Int. Immunol.* **11**, 1017-1025.
- Fiorini, E., Ferrero, I., Merck, E., Favre, S., Pierres, M., Luther, S. A. and MacDonald, H. R. (2008). Cutting edge: thymic crosstalk regulates delta-like 4 expression on cortical epithelial cells. *J. Immunol.* **181**, 8199-8203.
- Garbe, A. I., Krueger, A., Gounari, F., Zuniga-Pflucker, J. C. and von Boehmer, H. (2006). Differential synergy of Notch and T cell receptor signaling determines alphabeta versus gammadelta lineage fate. *J. Exp. Med.* **203**, 1579-1590.
- Garcia-Peydro, M., de Yebenes, V. G. and Toribio, M. L. (2003). Sustained Notch1 signaling instructs the earliest human intrathymic precursors to adopt a gammadelta T-cell fate in fetal thymus organ culture. *Blood* **102**, 2444-2451.
- Griffith, A. V., Fallahi, M., Nakase, H., Gosink, M., Young, B. and Petrie, H. T. (2009). Spatial mapping of thymic stromal microenvironments reveals unique features influencing T lymphoid differentiation. *Immunity* **31**, 999-1009.
- Haynes, B. F. and Heinly, C. S. (1995). Early human T cell development: analysis of the human thymus at the time of initial entry of hematopoietic stem cells into the fetal thymic microenvironment. *J. Exp. Med.* **181**, 1445-1458.
- Haynes, B. F., Sempowski, G. D., Wells, A. F. and Hale, L. P. (2000). The human thymus during aging. *Immunol. Res.* **22**, 253-262.
- Hoffman, E. S., Passoni, L., Crompton, T., Leu, T. M., Schatz, D. G., Koff, A., Owen, M. J. and Hayday, A. C. (1996). Productive T-cell receptor beta-chain gene rearrangement: coincident regulation of cell cycle and clonality during development in vivo. *Genes Dev.* **10**, 948-962.
- Hozumi, K., Negishi, N., Suzuki, D., Abe, N., Sotomaru, Y., Tamaoki, N., Mailhos, C., Ish-Horowitz, D., Habu, S. and Owen, M. J. (2004). Delta-like 1 is necessary for the generation of marginal zone B cells but not T cells in vivo. *Nat. Immunol.* **5**, 638-644.
- Hozumi, K., Mailhos, C., Negishi, N., Hirano, K., Yahata, T., Ando, K., Zuklys, S., Holländer, G. A., Shima, D. T. and Habu, S. (2008). Delta-like 4 is indispensable in thymic environment specific for T cell development. *J. Exp. Med.* **205**, 2507-2513.
- Jiang, R., Lan, Y., Chapman, H. D., Shawber, C., Norton, C. R., Serreze, D. V., Weinmaster, G. and Gridley, T. (1998). Defects in limb, craniofacial, and thymic development in Jagged2 mutant mice. *Genes Dev.* **12**, 1046-1057.
- Kang, J. and Raulet, D. H. (1997). Events that regulate differentiation of alpha beta TCR+ and gamma delta TCR+ T cells from a common precursor. *Semin. Immunol.* **9**, 171-179.
- Koch, U., Fiorini, E., Benedito, R., Besseyrias, V., Schuster-Gossler, K., Pierres, M., Manley, N. R., Duarte, A., Macdonald, H. R. and Radtke, F. (2008). Delta-like 4 is the essential, nonredundant ligand for Notch1 during thymic T cell lineage commitment. *J. Exp. Med.* **205**, 2515-2523.
- Lehar, S. M., Dooley, J., Farr, A. G. and Bevan, M. J. (2005). Notch ligands Delta 1 and Jagged1 transmit distinct signals to T-cell precursors. *Blood* **105**, 1440-1447.
- Lind, E. F., Prockop, S. E., Porritt, H. E. and Petrie, H. T. (2001). Mapping precursor movement through the postnatal thymus reveals specific microenvironments supporting defined stages of early lymphoid development. *J. Exp. Med.* **194**, 127-134.
- Lobach, D. F. and Haynes, B. F. (1987). Ontogeny of the human thymus during fetal development. *J. Clin. Immunol.* **7**, 81-97.
- Maillard, I., Tu, L. L., Sambandam, A., Yashiro-Ohtani, Y., Millholland, J., Keeshan, K., Shestova, O., Xu, L., Bhandoola, A. and Pear, W. S. (2006). The requirement for Notch signaling at the beta-selection checkpoint in vivo is absolute and independent of the pre-T cell receptor. *J. Exp. Med.* **203**, 2239-2245.
- Martin-Gayo, E., Gonzalez-Garcia, S., Garcia-Leon, M. J., Murcia-Ceballos, A., Alcaín, J., Garcia-Peydro, M., Allende, L., de Andres, B., Gaspar, M. L. and Toribio, M. L. (2017). Spatially restricted JAG1-Notch signaling in human thymus provides suitable DC developmental niches. *J. Exp. Med.* **214**, 3361-3379.
- Offner, F., Van Beneden, K., Debacker, V., Vanhecke, D., Vandekerckhove, B., Plum, J. and Leclercq, G. (1997). Phenotypic and functional maturation of TCR gammadelta cells in the human thymus. *J. Immunol.* **158**, 4634-4641.
- O'Neill, K. E., Bredenkamp, N., Tischner, C., Vaidya, H. J., Stenhouse, F. H., Peddie, C. D., Nowell, C. S., Gaskell, T. and Blackburn, C. C. (2016). Foxn1 is dynamically regulated in thymic epithelial cells during embryogenesis and at the onset of thymic involution. *PLoS ONE* **11**, e0151666.
- Ortmann, C. L., Dittmar, K. A., Witte, P. L. and Le, P. T. (2002). Molecular characterization of the mouse involuted thymus: aberrations in expression of transcription regulators in thymocyte and epithelial compartments. *Int. Immunol.* **14**, 813-822.
- Petrie, H. T. (2002). Role of thymic organ structure and stromal composition in steady-state postnatal T-cell production. *Immunol. Rev.* **189**, 8-19.
- Petrie, H. T. and Zúñiga-Pflücker, J. C. (2007). Zoned out: functional mapping of stromal signaling microenvironments in the thymus. *Annu. Rev. Immunol.* **25**, 649-679.
- Pui, J. C., Allman, D., Xu, L., DeRocco, S., Karnell, F. G., Bakkour, S., Lee, J. Y., Kadesch, T., Hardy, R. R., Aster, J. C. et al. (1999). Notch1 expression in early lymphopoiesis influences B versus T lineage determination. *Immunity* **11**, 299-308.
- Radtke, F., Wilson, A., Stark, G., Bauer, M., van Meerwijk, J., MacDonald, H. R. and Aguet, M. (1999). Deficient T cell fate specification in mice with an induced inactivation of Notch1. *Immunity* **10**, 547-558.
- Reis, M. D., Csomos, K., Dias, L. P., Prodan, Z., Szerafin, T., Savino, W. and Takacs, L. (2015). Decline of FOXP1 gene expression in human thymus correlates with age: possible epigenetic regulation. *Immun. Ageing* **12**, 18.
- Schmitt, T. M., Ciofani, M., Petrie, H. T. and Zúñiga-Pflücker, J. C. (2004). Maintenance of T cell specification and differentiation requires recurrent notch receptor-ligand interactions. *J. Exp. Med.* **200**, 469-479.
- Shimizu, K., Chiba, S., Saito, T., Kumano, K., Hamada, Y. and Hirai, H. (2002). Functional diversity among Notch1, Notch2, and Notch3 receptors. *Biophys. Res. Commun.* **291**, 775-779.
- Takahama, Y. (2006). Journey through the thymus: stromal guides for T-cell development and selection. *Nat. Rev. Immunol.* **6**, 127-135.
- Tanigaki, K., Tsuji, M., Yamamoto, N., Han, H., Tsukada, J., Inoue, H., Kubo, M. and Honjo, T. (2004). Regulation of alphabeta/gammadelta T cell lineage commitment and peripheral T cell responses by Notch/RBP-J signaling. *Immunity* **20**, 611-622.
- Van de Walle, I., De Smet, G., De Smedt, M., Vandekerckhove, B., Leclercq, G., Plum, J. and Taghon, T. (2009). An early decrease in Notch activation is required for human TCR-alphabeta lineage differentiation at the expense of TCR-gammadelta T cells. *Blood* **113**, 2988-2998.
- Van de Walle, I., De Smet, G., Gartner, M., De Smedt, M., Waegemans, E., Vandekerckhove, B., Leclercq, G., Plum, J., Aster, J. C., Bernstein, I. D. et al. (2011). Jagged2 acts as a Delta-like Notch ligand during early hematopoietic cell fate decisions. *Blood* **117**, 4449-4459.
- Van de Walle, I., Waegemans, E., De Medts, J., De Smet, G., De Smedt, M., Snauwaert, S., Vandekerckhove, B., Kerre, T., Leclercq, G., Plum, J. et al. (2013). Specific Notch receptor-ligand interactions control human TCR-alphabeta/gammadelta development by inducing differential Notch signal strength. *J. Exp. Med.* **210**, 683-697.
- Witt, C. M. and Robbins, K. (2005). Tracking thymocyte migration in situ. *Semin. Immunol.* **17**, 421-430.

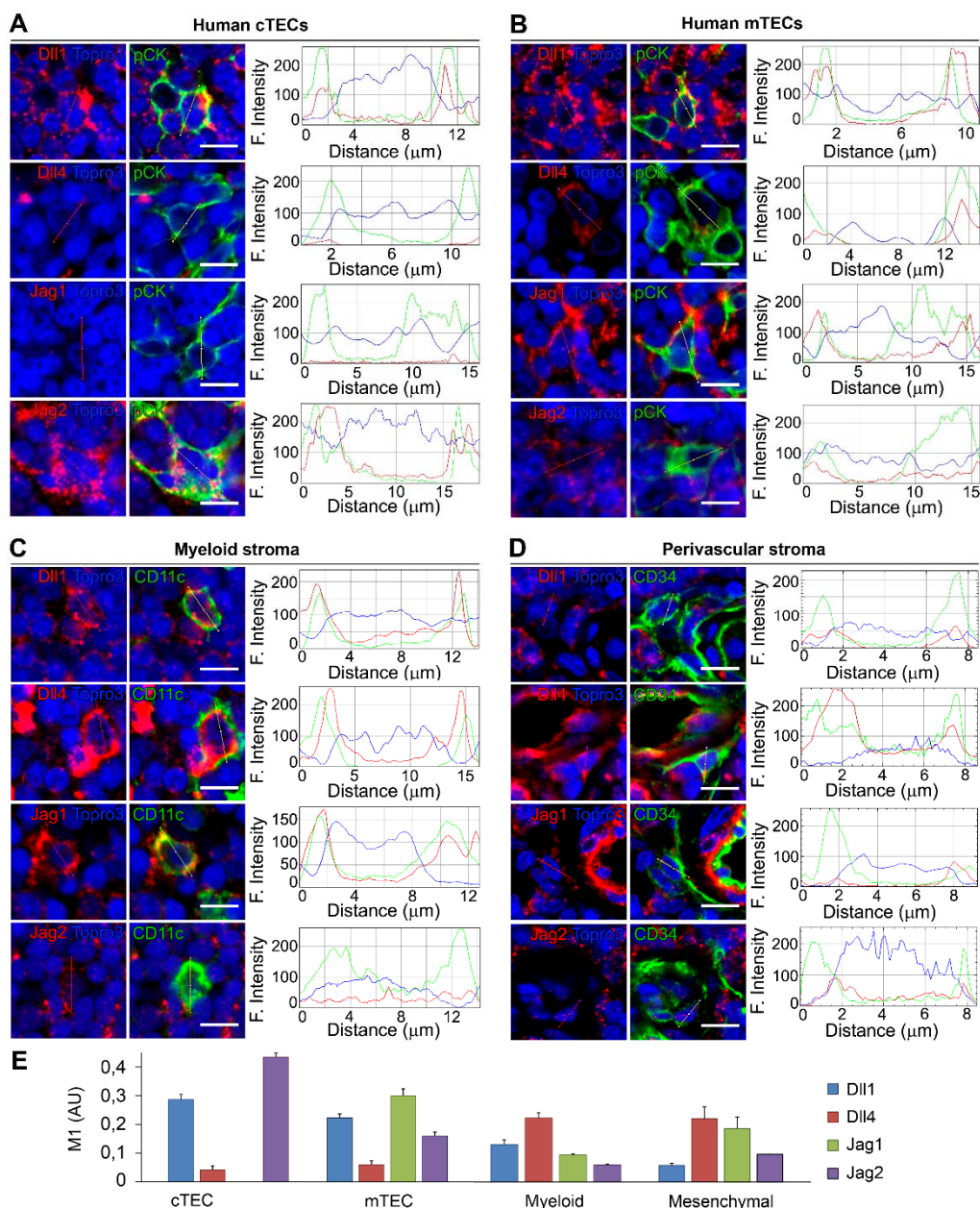


Figure S1. Co-localization analyses of Notch ligands with stromal cells in the human postnatal thymus. (A-D) Image ROIs (30 μ m) of postnatal human thymus sections labelled with anti-Notch ligand antibodies showing single stromal cells, including cTECs (A), mTECs (B), CD11c⁺ (C) and CD34⁺ (D) and its corresponding RGB colocalization profile. RGB mean fluorescence intensity (MFI) of single stromal cells was measured by tracing a linear ROI (yellow line) along the cells. Images are representative of results obtained from at least 3 different tissue samples per ligand and stromal marker. Scale bars: 10 μ m. (E) Graph bars show M1 co-localization of Mander's coefficient. ICA plugin (Li et al., 2004) was applied to at least 10 images of cortical and medullary areas for each stromal marker and Notch ligand, obtained from different tissue samples (n=3).

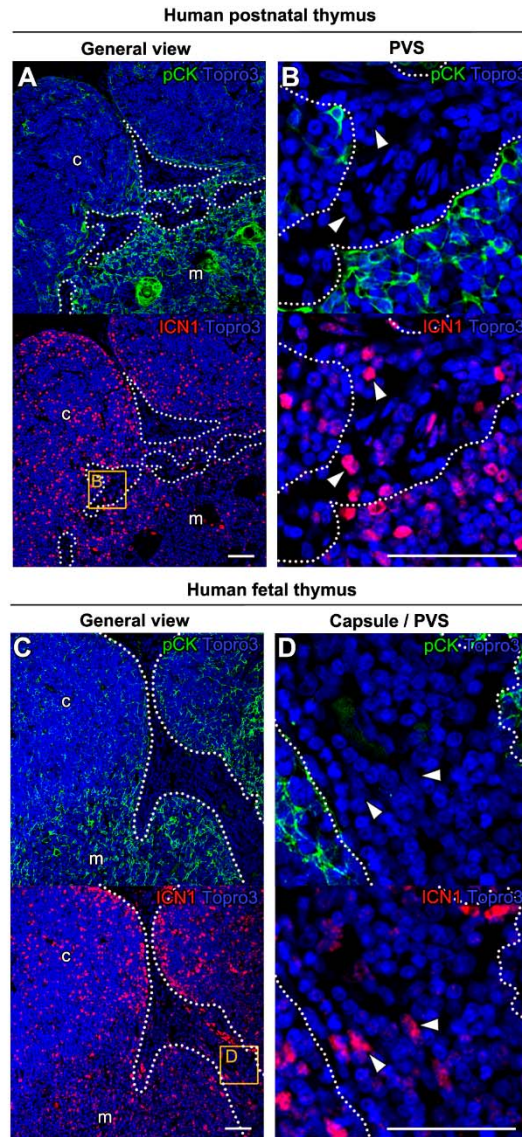


Figure S2. ICN1+ cells are located at extraparenchymal areas including the PVS and the interlobular capsule of the human postnatal and fetal thymus. Immunohistochemistry of active intracellular Notch1 (ICN1, red) and pCK (green), with nuclei labelled in blue (Topro3). *c*: cortex; *m*: medulla; *dotted line*: thymic capsule / PVS, which is pCK- and shows low cellularity (Topro3). General (A) and detailed view (B) of ICN1 expression in the human postnatal thymus. General (C) and detailed view (D) of ICN1 expression in the human fetal thymus. Arrowheads show extraparenchymal thymocytes expressing nuclear ICN1. Scale bar: 50µm. Images are representative of more than 10 images per thymus sample (n=3).

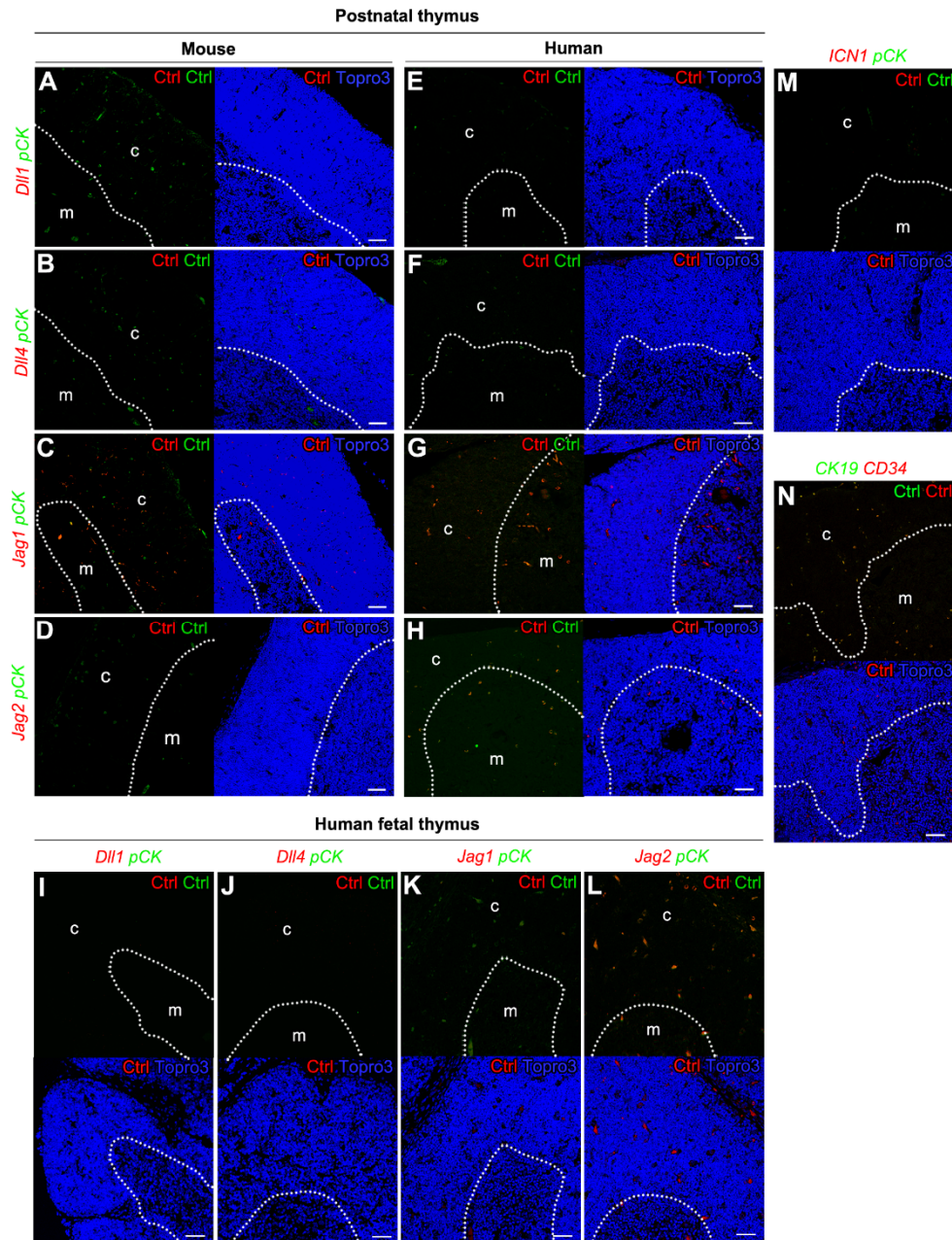


Figure S3. Immunohistochemistry controls of murine and human thymic tissue. FFPE sections of mouse (< 16 weeks-old) and human (< 17 months-old) postnatal thymus samples or human fetal thymus (11-19 weeks) were untreated or treated with isotype-matched irrelevant antibodies and then incubated with secondary reagents. Topro3 shows nuclear staining (blue). *c*: cortex; and *m*: medulla; *dotted line*: CMJ; *h*: Hassal's corpuscles. Images are representative of results obtained from at least 10 images from 2-3 different samples. Scale bars: 50µm.